Int J Thermophys (2017) 38:137
DOI 10.1007/s10765-017-2272-0

TEMPMEKO 2016

Effects of Beryllium and Compaction Pressure on the Thermal Diffusivity of Uranium Dioxide Fuel Pellets

D. M. Camarano[1] · F. A. Mansur[1] · A. M. M. Santos[1] · W. B. Ferraz[1] · R. A. N. Ferreira[1]

Received: 29 June 2016 / Accepted: 14 July 2017 / Published online: 25 July 2017

Abstract In nuclear reactors, the performance of uranium dioxide (UO_2) fuel is strongly dependent on the thermal conductivity, which directly affects the fuel pellet temperature, the fission gas release and the fuel rod mechanical behavior during reactor operation. The use of additives to improve UO_2 fuel performance has been investigated, and beryllium oxide (BeO) appears as a suitable additive because of its high thermal conductivity and excellent chemical compatibility with UO_2. In this paper, UO_2–BeO pellets were manufactured by mechanical mixing, pressing and sintering processes varying the BeO contents and compaction pressures. Pellets with BeO contents of 2 wt%, 3 wt%, 5 wt% and 7 wt% BeO were pressed at 400 MPa, 500 MPa and 600 MPa. The laser flash method was applied to determine the thermal diffusivity, and the results showed that the thermal diffusivity tends to increase with BeO content. Comparing thermal diffusivity results of UO_2 with UO_2–BeO pellets, it was observed that there was an increase in thermal diffusivity of at least 18 % for the UO_2-2 wt% BeO pellet pressed at 400 MPa. The maximum relative expanded uncertainty (coverage factor k = 2) of the thermal diffusivity measurements was estimated to be 9 %.

Keywords Beryllium oxide · Laser flash method · Thermal diffusivity · Uranium dioxide

Selected Papers of the 13th International Symposium on Temperature, Humidity, Moisture and Thermal Measurements in Industry and Science.

✉ D. M. Camarano
dmc@cdtn.br

[1] Centro de Desenvolvimento da Tecnologia Nuclear, CDTN, Belo Horizonte, MG 31270-901, Brazil

1 Introduction

The UO_2 pellet is the most used fuel in LWR (light-water reactor) due to its characteristics such as high chemical and physical stabilities, high melting point and capacity of fission product retention. The performance of this fuel is strongly dependent on the thermal conductivity, which directly affects the fuel pellet temperature, the fission gas release and the fuel rod mechanical behavior during reactor operation. The use of additives to improve the UO_2 fuel performance is promising as shown in the literature [1–5]. The UO_2 nuclear fuel can have its thermal conductivity increased with the addition of a second material with a higher thermal conductivity in relation to the UO_2 and chemically compatible with UO_2 as the beryllium oxide (BeO) [6–9]. This paper describes the process of obtaining UO_2 pellets with addition of BeO pressed at different compaction pressures based on the conventional UO_2 pellets manufacturing processes such as mixing, pressing, and sintering under reducing atmosphere. The mixed oxides of uranium and beryllium were obtained with 2 wt%, 3 wt%, 5 wt% and 7 wt% of BeO, and UO_2 pellets were also obtained for comparing. The green and sintered densities of fuel pellets were determined by geometric and immersion [10] methods, respectively. Microstructural characterization was carried out using scanning electron microscopy (SEM) and energy-dispersive spectroscopy (EDS). The thermal diffusivity of UO_2–BeO pellets was determined by laser flash method [11], and the expanded uncertainty was estimated according to the ISO/BIPM Guide to the Expression of Uncertainty in Measurement (GUM) [12]. The relationship between thermal diffusivity and beryllium oxide content under different compaction pressures was investigated.

2 Experimental Apparatus and Procedures

2.1 Pellets Fabrication

Uranium and beryllium oxides were mixed in a rotary mechanical mixer for 3 h, and BeO contents of the powder mixtures were 2 wt%, 3 wt%, 5 wt% and 7 wt% or 6.9 vol%, 10.1 vol%, 16.0 vol% and 21.5 vol%, respectively. Each powder batch prepared was pressed under compaction pressures of 400 MPa, 500 MPa and 600 MPa. A double-action hydraulic press was utilized, and the diameter of the green pellets was about 11 mm. The pellets thickness ranged from 2.1 mm to 2.4 mm. These green pellets were sintered at 1750 °C for 3 h in a horizontal furnace under Ar/H_2 atmosphere. UO_2 fuel pellets were also obtained in these same conditions for comparison with fuel UO_2–BeO pellets. A total of 45 pellets were obtained, of which 15 pellets were used for density determination and microstructural characterization.

2.2 Pellets Density

The geometric density of the green pellets was determined using a micrometer and an analytic balance with resolutions of 10^{-3} mm and 10^{-4} g, respectively. The density of the sintered pellets was determined by penetration-immersion method based on

Archimedes' principle using xylol as immersion liquid [10]. This method has higher precision and accuracy than the geometrical method.

2.3 Microstructural Examination

Microstructural aspects such as pores, precipitates, cracks and grains of the sintered pellets were examined using an optical microscopy (Leica, DM4500P) and a scanning electron microscopy (Carl Zeiss, Sigma VP) equipped with energy-dispersive X-ray spectroscopy—EDS (Bruker, XFlash 4.0). The EDS analyses were performed to identify the BeO precipitates. Microstructure was observed on samples prepared by usual metallography technique as cutting, resin embedding, grinding and polishing. The smooth sample surfaces were achieved using SiC papers with sequential grit sizes from 300 to 600 and diamond pastes (3 μm and 1 μm). To reveal the grain structure some samples were thermally etched at 1200 °C for 2 h in a CO/CO_2 atmosphere.

2.4 Thermal Diffusivity

Thermal diffusivity was determined by laser flash method at room temperature according to ASTM E-1461-13 [13], and the pellets were considered macroscopically homogeneous. By this method, the front face of a small disk-shaped sample is subjected to a very short burst of radiant energy. The source of the radiant energy is a CO_2 laser, and the irradiation times are of the order of milliseconds. A thermogram is obtained from the temperature increase on the sample rear surface, and the thermal diffusivity is calculated by Eq. 1:

$$\alpha = \frac{1.37 \cdot L^2}{\pi^2 \cdot t_{1/2}}, \tag{1}$$

where α is the sample thermal diffusivity ($m^2 \cdot s^{-1}$), L is the sample thickness (m), and $t_{1/2}$ is the half-time (s).

In order to consider the correlation with porosity, the thermal diffusivity was normalized to 95 % of theoretical density (TD) according to [6]. Figure 1 shows the schematic diagram of laser flash method utilized in LMPT (Thermophysical Properties Measurement Laboratory). The CO_2 laser (10.6 μm wavelength) equipment (Bioluz, BL 80i) has a maximal power output of 80 W. The temperature was measured by a calibrated optical infrared detector (Raytek, RAYMMLTSSF1L). The temperature rise signal versus time was amplified and recorded using a calibrated 16 bits A/D converter (National Instruments, USB-6251). The built-in furnace has a heat element of platinum/30 % rhodium, and its chamber can be heated up to 1700 °C. The measurements were taken with duration of the laser pulse of 15 ms, and the sample rear face temperature rise was limited to a maximal value of 3 °C. The pellets were coated with carbon film on both faces to improve the emissivity and absorptivity, and the emissivity was estimated to be 0.90. The uncertainty sources of the thermal diffusivity determination are associated with the sample itself, the temperature and time measurements, the

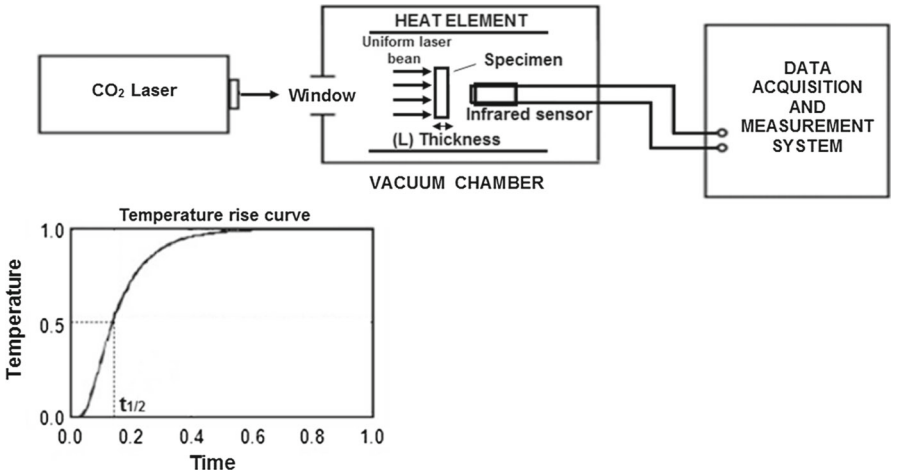

Fig. 1 Schematic diagram of laser flash method of the thermophysical properties measurement laboratory

sample non-uniform heating, heat losses and the finite pulse time effect. These sources of uncertainties were considered according to [14]. The reliability of measurements was checked by comparing the measured temperature rise versus time curve with the analytical curve. Moreover, in order to check the accuracy of the thermal diffusivity determination system we used as reference a graphite standard [15]. In addition, an Inconel 600 standard [16] was also used to verify the performance of the experimental apparatus considering that its thermal diffusivity is of same order of magnitude of the UO_2–BeO pellets. The maximum deviation of reference and obtained values of thermal diffusivity was 4 % and 2 % for the graphite standard and Inconel 600 standard, respectively. These deviations were within the uncertainty of the reference values.

3 Results

3.1 Pellet Fuel Fabrication

The green and sintered densities of UO_2 and UO_2–BeO pellets at different compaction pressures are listed in Table 1. The theoretical density (TD) of the pellets is also given in Table 1. Figure 2 shows the density of sintered pellets as a function of compaction pressure for each BeO content. It was observed that the density of sintered pellets was strongly dependent on the BeO content. A slight increase in pellet densities for the compaction pressures of 500 MPa and 600 MPa was observed as compared to 400 MPa for all BeO contents, with the exception of the pellets containing 7 wt% BeO pressed at 400 MPa and 500 MPa. This is probably due to the presence of cracks generated under higher compaction pressure associated with a higher content of BeO. The maximum relative expanded uncertainty (coverage factor k = 2) was estimated to be 2 %.

Table 1 Data for UO_2 and UO_2–BeO fuel pellets

Compaction pressure (MPa)	BeO (wt%)	BeO (vol%)	Green density ($g \cdot cm^{-3}$)	Sintered density ($g \cdot cm^{-3}$)	TD ($g \cdot cm^{-3}$)	%TD
400	0	0	6.03	10.27	10.96	93.80
	2	6.9	5.67	9.93	10.41	95.86
	3	10.1	5.54	9.76	10.24	92.02
	5	16.0	5.23	9.13	9.72	95.03
	7	21.5	4.99	8.76	9.29	94.44
500	0	0	6.15	10.55	10.96	94.03
	2	6.9	5.77	10.02	10.41	95.73
	3	10.1	5.55	9.80	10.24	96.05
	5	16.0	5.48	9.27	9.72	95.66
	7	21.5	5.14	8.77	9.29	95.33
600	0	0	6.23	10.58	10.96	94.64
	2	6.9	5.86	10.01	10.41	96.94
	3	10.1	5.75	9.79	10.24	96.40
	5	16.0	5.63	9.33	9.72	95.71
	7	21.5	5.20	8.73	9.29	96.44

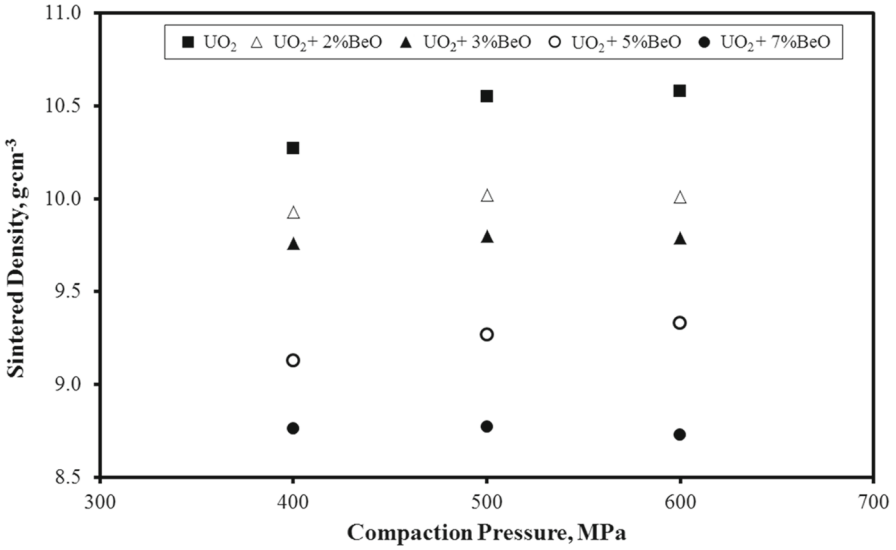

Fig. 2 Sintered pellet density as a function of the compaction pressure

3.2 Microstructural Examination

Microstructural analysis of the pellets with BeO pressed at different compaction pressures shows similar microstructures with precipitates and pores. SEM micrographs of

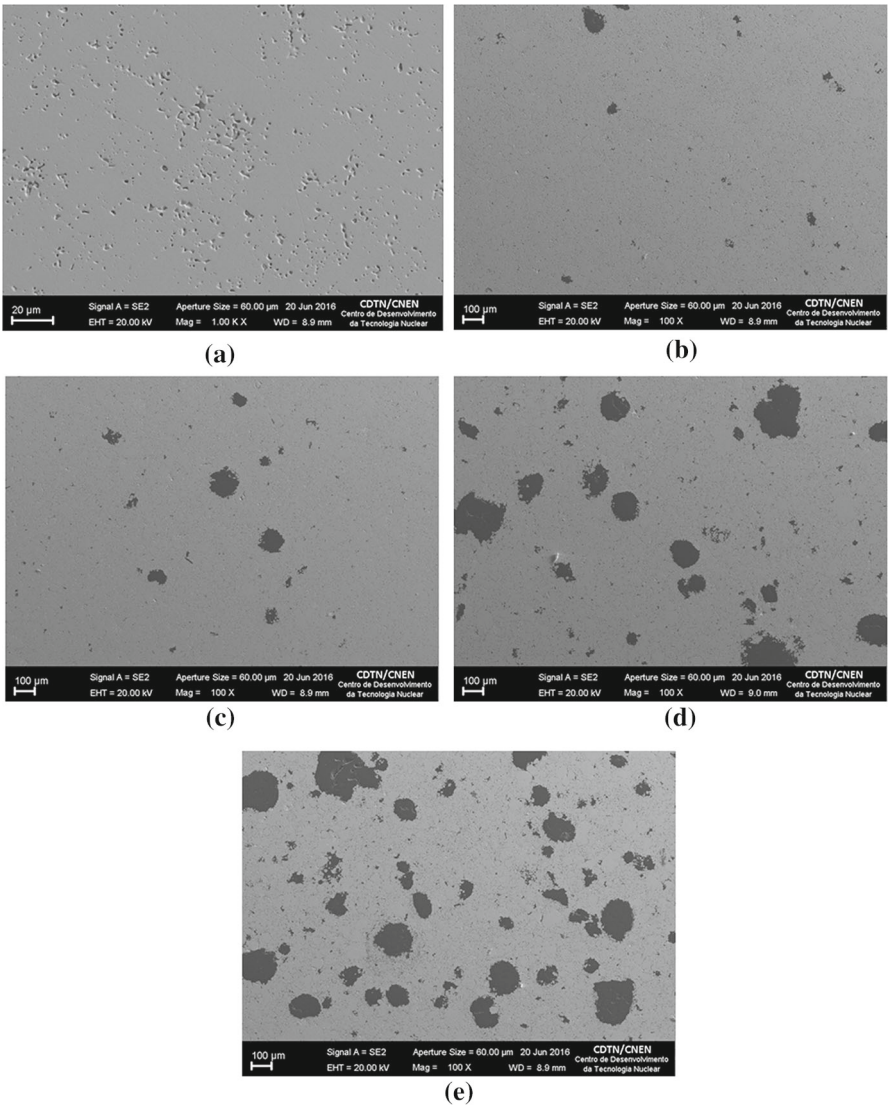

Fig. 3 SEM micrographs of UO_2 and UO_2–BeO pellets pressed at 400 MPa: (a) UO_2, (b) UO_2–2 wt% BeO, (c) UO_2–3 wt% BeO, (d) UO_2–5 wt% BeO, (e) UO_2–7 wt% BeO

the UO_2 and UO_2–BeO pellets pressed at 400 MPa are shown in Fig. 3. EDS analyses by elements mapping were also carried out in the pellets. It was observed that UO_2 and BeO phases are present without forming a solid solution, as observed by Ishimoto et al. [6]. The pellets with 2 wt% and 3 wt% of BeO show smaller precipitates at all compaction pressures. Furthermore, the values of density of these pellets are within the range of UO_2 pellet project specification (95 $\pm$ 1.5 %TD). For the UO_2–3 wt% BeO pellets, a higher quantity of BeO precipitates was verified. Typical grain structures of

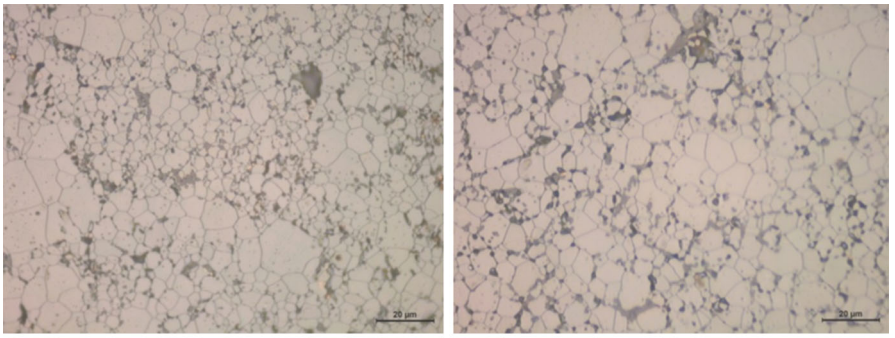

Fig. 4 Thermally etched microstructure of the UO_2 and UO_2–5 wt% BeO pellets pressed at 400 MPa: (a) UO_2 and (b) UO_2–5 wt% BeO

UO_2 and UO_2–BeO for compaction pressure of 400 MPa are shown in Fig. 4. It was observed that the presence of beryllium oxide did not change the grain structure of the pellets. The UO_2 pellets showed large and small grains with the same aspects of the pellets containing BeO, as shown in Fig. 4. In the mechanical mixing process of UO_2 and BeO powders, the BeO particles tend to agglomerate and do not modify the grain structure in the pellets containing up to 5 wt% BeO.

3.3 Thermal Diffusivity

Thermal diffusivities results are presented in Table 2. Figure 5 shows the thermal diffusivity of the pellets versus compaction pressure for different contents of beryllium oxide. The thermal diffusivity values were achieved on repeatability conditions from 5 measurements. The maximum relative expanded uncertainty (coverage factor k = 2) was estimated to be 9 %. As can be seen, the thermal diffusivity of the pellets increased significantly with BeO addition. The maximum difference between the results of thermal diffusivity in duplicate samples was less than 2.5 %, indicating there is a good similarity between them. Also, there was no significative difference in the thermal diffusivity values in relation to compaction pressure. For compaction pressure of 400 MPa, the UO_2 thermal diffusivity mean value was 2.99×10^{-6} $m^2 \cdot s^{-1}$ and for UO_2 with addition of 2 wt%, 3 wt%, 5 wt% and 7 wt% BeO, was 3.52, 3.70, 4.03 and 4.41×10^{-6} $m^2 \cdot s^{-1}$, respectively. Each of these values represents an increase in thermal diffusivity corresponding to 18 %, 24 %, 35 % and 48 % as compared to UO_2. Considering the normalized thermal diffusivities to 95 % TD, these values changed to 16 %, 29 %, 33 % and 46 %, respectively. For the other compaction pressures the thermal diffusivity results show a similar behavior. The thermal diffusivity was practically constant for 5 wt% and 7 wt% BeO even with the increase in the compaction pressure. By the microstructural evaluation, a greater amount of precipitate was observed in the pellets with these BeO contents that may have contributed to this behavior. Ishimoto et al. [6] studied pellets from a mixture of UO_2 and BeO powders containing 0.3 wt%, 0.6 wt%, 0.9 wt%, 1.2 wt% and 13.6 wt% BeO, pressed at 300 MPa and sintered under

Table 2 Thermal diffusivity of UO_2 and UO_2–BeO pellets at different compaction pressures

BeO (wt%)	Compaction pressure (MPa)					
	400		500		600	
	Thermal diffusivity (10^{-6} $m^2 \cdot s^{-1}$)	Expanded uncertainty $U_{95\,\%}$ (10^{-6} $m^2 \cdot s^{-1}$)	Thermal diffusivity (10^{-6} $m^2 \cdot s^{-1}$)	Expanded uncertainty $U_{95\,\%}$ (10^{-6} $m^2 \cdot s^{-1}$)	Thermal diffusivity (10^{-6} $m^2 \cdot s^{-1}$)	Expanded uncertainty $U_{95\,\%}$ (10^{-6} $m^2 \cdot s^{-1}$)
0	3.00	0.25	3.03	0.24	3.03	0.23
0	2.97	0.26	3.05	0.25	3.12	0.24
2	3.57	0.32	3.72	0.26	3.75	0.31
2	3.47	0.29	3.67	0.30	3.67	0.29
3	3.65	0.33	3.81	0.31	3.83	0.30
3	3.74	0.34	3.83	0.29	3.79	0.34
5	3.98	0.34	4.01	0.34	4.00	0.33
5	4.07	0.32	4.11	0.33	4.09	0.35
7	4.43	0.35	4.44	0.36	4.46	0.38
7	4.39	0.36	4.39	0.38	4.57	0.35

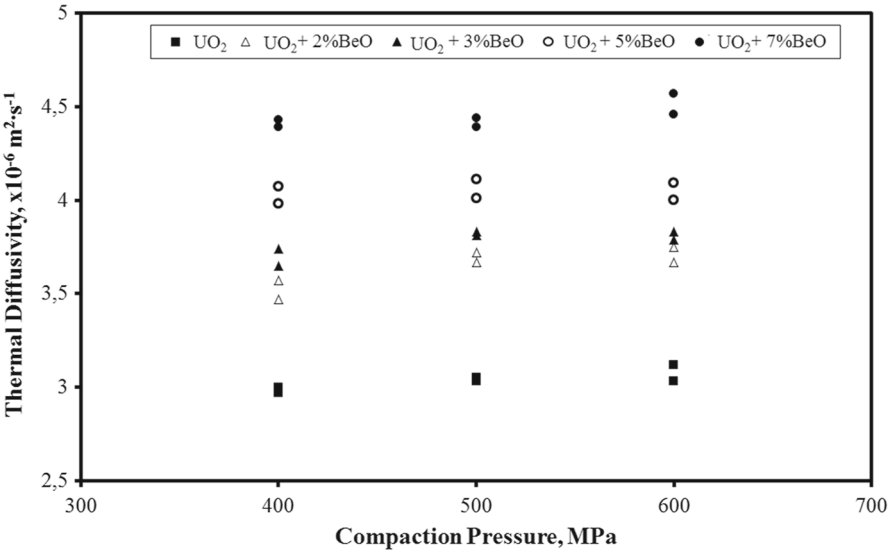

Fig. 5 Thermal diffusivity as a function of compaction pressure for UO_2 and UO_2–BeO pellets

reducing atmosphere. They also observed that thermal diffusivity value of UO_2–BeO pellets increased with BeO content. The obtained results emphasize that the BeO is a promising material to improve the thermal performance of UO_2 nuclear fuel as also observed in the literature [2,6–9].

4 Conclusions

UO_2–BeO pellets were obtained with different BeO contents and compaction pressures. It was observed that BeO particles were dispersed in the UO_2 matrix. An increase in the thermal diffusivity was verified with an increase in the beryllium oxide content. In relation to the compaction pressures of 400 MPa and 500 MPa there was a slight increase in thermal diffusivity for pellets containing 2 wt% and 3 wt% BeO. For pellets with 5 wt% and 7 wt% BeO contents no significant change in thermal diffusivity with the compaction pressure was observed. These results show that among the compaction pressures investigated the value of 400 MPa can be considered the better option to obtain UO_2–BeO nuclear fuel pellets, because this pressure is used in the commercial fuel fabrication and therefore will not impact on the fuel cost. The UO_2 thermal diffusivity mean value for compaction pressure of 400 MPa was 2.99×10^{-6} $m^2 \cdot s^{-1}$ and for UO_2 with addition of 2 wt%, 3 wt%, 5 wt% and 7 wt% BeO, was 3.52, 3.70, 4.03 and 4.41×10^{-6} $m^2 \cdot s^{-1}$, respectively. Therefore, there is an increase in the thermal diffusivity of 18 %, 24 %, 35 % and 48 % compared to UO_2. The obtained data at room temperature in this work can be seen as referential to measurements at higher temperatures.

Acknowledgements The authors thank the financial support of CNPq—Conselho Nacional de Desenvolvimento Científico e Tecnológico, SIBRATEC Rede GTD—Rede de Serviços Tecnológicos em Geração, Transmissão e Distribuição de Energia Elétrica and INCTRNi—Instituto Nacional de Ciência e Tecnologia de Reatores Nucleares Inovadores.

References

1. A.A. Kovalishina, V.N. Prosyolkova, V.D. Sidorenkoa, Y.V. Stogovb, Phys. At. Nucl. **77**, 1661 (2014)
2. D.S. Li, H. Garmestani, J. Schwartz, J. Nucl. Mat. **392**, 22 (2009)
3. W. Zhou, R. Liu, S.T. Revankar, Ann. Nucl. Energy **81**, 240 (2015)
4. A.A. Solomon, S. Revankar, J.K. McCoy, Enhanced thermal conductivity oxide fuels. (Project N°. 02-1802005, Award N° DE-FG07-02SF22613, 2005), http://www.osti.gov/scitech/servlets/purl/862369-iDA0bI/. Accessed 07 June 2016
5. IAEA, Thermophysical properties database of materials for light water reactors and heavy water reactors. (TECDOC 1496, 2006), http://www.pub.iaea.org/MTCD/publications/PDF/te_1496_web.pdf. Accessed 14 June 2016
6. S. Ishimoto, M. Hirai, K. Ito, Y. Korei, J. Nucl. Sci. Tech. **33**, 134 (1996)
7. K. McCoy, C. Mays, J. Nucl. Mat. **375**, 157 (2008)
8. S.K. Kim, W.I. Ko, H.D. Kim, S.T. Revankar, W. Zhou, D. Jo, J. Nucl. Mat. **52**, 813 (2010)
9. D. Chandramouli, S.T. Revankar, Int. J. Nucl. Energy **2014**, 751070 (2014). doi:10.1155/2014/751070
10. G. Maier, *Dichte und Porositätsmessung nach der Penetrations-Imersions Methode: Überprüfung und Möglichkeiten zur Verbesserung* (Kraftwerk Union (Arbeits-Bericht), Erlangen, 1978)
11. W.J. Parker, R.J. Jenkins, C.P. Butler, G.L. Abbot, J. Appl. Phys. **9**, 1679 (1961)
12. JCGM, *Evaluation of measurement data—guide to the expression of uncertainty in measurement*, JCGM 100:2008 (Joint Committee for Guides in Metrology, 2008)
13. ASTM E1461-13, *Standard Test Method for Thermal Diffusivity by the Flash Method*. (ASTM International, West Conshohocken, 2013). doi:10.1520/E1461
14. D.M. Camarano, F.L. Migliorini, E.H.C. Silva, P.A. Grossi, W.B. Ferraz, J.B. de Paula, Int. J. Themophys. **31**, 1842 (2010)
15. LNE, in *Test Report, Laboratorie National de Mëtrologie et D'Essais, Graphite Sample* (2009)
16. NETZSCH Gerätebau GmbH Applications Laboratory, in *Manufacture's Certification, Thermophysical Properties Standard, Inconel 600 Sample* (2009)